

OpenSim upper-extremity modelling: subject-specific scaling- and validation tools

J.M. de Vet (4375092)

Delft University of Technology, Faculty of 3mE, Mekelweg 2, 2628 CD Delft

March 12, 2021

Abstract—Muscle-driven simulations performed with a musculoskeletal model of the human upper-extremity need to include closed-loop kinematics to capture the limb’s full mobility and model the actions of thoracoscapular muscles. On the OpenSim platform, a single upper-extremity model with closed-loop kinematics is available: the thoracoscapular shoulder model (TSM), which only includes muscle-elements crossing the shoulder-girdle, omitting upper-extremity musculature partially. OpenSim’s native algorithms for subject-specific scaling of geometric- and muscle-length parameters function insufficiently for upper-extremity models, whilst inertial- and muscle-strength parameters are rarely scaled. Subject-specific models are impossible to validate *in vivo*, whilst indirect validation methods are limited.

The goal of this study is to enable future OpenSim users to perform muscle-driven simulations with adequately scaled, subject-specific upper-extremity models. This study develops: (1) A generic model with the closed-loop kinematic structure of the TSM and all upper-extremity musculature: the thoracoscapular Delft shoulder and elbow model (TDSEM). (2) Subject-specific scaling tools for the TSM and TDSEM, performing geometric- and muscle-length parameter scaling based on optimization procedures, and inertial- and muscle-strength scaling based on a total muscle-volume estimation. (3) A method to estimate maximum isometric directional force at an end-effector with subject-specific models to indirectly validate the maximum force-generating capacity of these models.

Geometric scaling accuracy is mainly limited by the accuracy of marker-data used. Both the TSM and TDSEM reached the desired RMS marker-error of ≤ 2 cm and an average segmental-length error of $\leq 5\%$. Muscle-length parameter optimization fit is comparable to, or better than, studies employing similar algorithms. Scaled muscle-strength-, and inertial parameters are not validated, but the accuracy of the muscle-volume estimates they are derived from was known beforehand. The indirect validation method is not able to make estimations within $\pm 10\%$ of measured maximum forces. The method greatly overestimates measured values, regardless of the subject modelled or model used.

Including upper-extremity musculature in the TDSEM results in improved muscle-driven analyses compared to the TSM. This can be improved further by improving the accuracy of muscle-elements attached to the radius, including ligaments in the model, and using a constraint to maintain glenohumeral stability. The presented scaling methods are recommended over OpenSim’s native methods when scaling the TSM or TDSEM. The indirect validation method must be improved before it can be used to inform (in)validating conclusions about subject-specific models. For this, the effect of a constrained torso, task-specific practice, and inclusion of trained subjects on measurements must be evaluated and subject pose must be recorded. When combined with the stability constraint, estimation accuracy will likely improve greatly.

I. INTRODUCTION

A. Background

Musculoskeletal (MSK) modelling enables the study of numerous aspects of human movement and biomechanics that cannot be measured: providing insight into mechanical work performed by muscles and loads experienced by joints or predict kinematic adaptations resulting from pathologies and surgical interventions [1]–[4]. MSK models subdivide into skeletal-, joint-, muscle-, and neural models, each describing different aspects of the biological system [5]. Commonly, specialized modelling software – like OpenSim [6]–[8] or AnyBody [9], [10] – is used.

MSK models of the human upper-extremity need to capture the complex motion of the shoulder girdle resulting from simultaneous articulations between thorax, clavicle, scapula, and humerus. For this purpose, open-loop-, closed-loop-, and coupled kinematic models have been developed [11]–[14]. In open-loop kinematic models, the sternoclavicular- (SC) and acromioclavicular (AC) joint move independently. Closed-loop kinematic models relate SC- and AC-joint movement by constraining scapular motion to a surface representing the thorax: a scapulothoracic (ST) joint. In coupled kinematic models, scapular and clavicular motion is estimated as a function of humeral motion, obtained using regressions.

Generic models are MSK models constructed from cadaveric data. Measuring all MSK parameters in a model requires dissection. Cadaveric data either contains averaged data from multiple specimens, or a fully consistent dataset obtained from a single, typical specimen. To date, a single, fully consistent upper-extremity dataset is published [15], [16]. Generic upper-extremity models employing open-loop, closed-loop, and coupled kinematic models are available on the OpenSim platform [14], [17]–[22].

When modelling the behavior of a single subject, parameters in a generic model are adjusted based on subject-specific data obtained *in vivo* to account for the morphological differences between the subject and the cadaveric data contained in the generic model. It is assumed with subject-specific modelling that this partial integration improves model validity, regardless of hereby introduced inconsistencies in the model’s dataset [5]. The value of parameter personalization is determined by; the task-dependent *sensitivity* of simulation results to variation in a parameter [23]–[36], the inter-individual *variability* of a parameter [37]–[44], and the

parameter's *measurability* – given by the costs and accuracy of *in vivo* measurement [5]. Current subject-specific scaling methods fall into one of four categories:

- *Geometric scaling* adjusts joint- and muscle-attachment site locations in the skeletal model. Commonly, this is based on medical imaging or marker data [2], [45]–[55].
- *Muscle-length scaling* adjust the length-dependent properties in the Hill-type [56], [57] muscle-model: optimal fiber length and tendon slack length. Both parameters are highly influential and troublesome to measure *in vivo* [28], [29]. As such, it is currently best practice to maintain the normalized operating range – defined by these parameters – of the generic model's muscles in a scaled model through the use of an optimization algorithm [58]–[60].
- *Muscle-strength scaling* adjusts the maximum isometric muscle-force parameter in the Hill-type muscle-model. This parameter is estimated using measured muscle-volumes or maximum isometric and/or isokinetic strength trials [61]–[66].
- *Inertial scaling* adjust the translational and rotational inertias in the skeletal model. This is based on medical imaging or regressions [43], [67], [68].

The joint- and neural models are not adjusted with subject-specific scaling.

B. Problem statements

Problem 1: Muscle-driven simulations of the upper-extremity need to capture the contribution of the scapula to the multibody dynamics. To also capture the independent mobility of the scapula, a closed-loop kinematic structure is thus required [14], [69]. One generic MSK model employing a closed-loop kinematic structure is currently available in OpenSim: the thoracoscapular shoulder model (TSM) by Seth et al. [14], [17]. In the TSM, only muscles crossing the shoulder-girdle are modelled. There is no model available in OpenSim containing both a closed-loop kinematic structure and a complete and consistent dataset of the human upper extremity. There is one generic model that has both these attributes: the Delft shoulder and elbow model (DSEM) [15], [16], [70]–[72]. The DSEM has not yet been implemented in OpenSim.

Problem 2: A recommended set of subject-specific scaling methods, compatible with closed-loop upper-extremity models in OpenSim, is not available. OpenSim's native scaling-tool uses marker-based, Cartesian scale-factors. This scaling-algorithm is insufficient when used for upper-extremity models, leading to the use of a custom, unpublished optimization algorithm by Seth et al. [17]. The muscle-length scaling algorithm published by Modenese et al. [59] is incompatible with later releases of OpenSim (4.0 and later) and highly inefficient for open- and closed-loop upper-extremity models due to their large mobility. Muscle-strength scaling is rarely performed based on subject-specific measurements, often omitting a subject's force-generating-capacity from subject-specific models, even though it is highly variable between subjects [41], [65], [73].

Problem 3: Muscle-forces predicted with subject-specific MSK models cannot be validated *in vivo*. Instrumented joint prosthesis can be used to compare model predicted- and measured joint-loads, indirectly validating model predictions [54], [70], [74]–[77]. This strategy cannot be used when modelling non-instrumented subjects. Electromyography (EMG) is commonly used for indirect validation by comparing predicted muscle-contractions with measured EMG activity, or motion- or force measurements to EMG-driven model-predictions [78]–[84]. Yet, EMG recordings do not always linearly correspond to muscle-forces, cannot be easily acquired for all muscles, and can be erroneous [5], [85], [86], leading to large corrections required in EMG-driven simulations [87]. Bolsterlee [5] suggested another method for indirect validation of subject-specific models: comparing model-predicted- and measured maximum externally exerted forces in different poses and directions. This method is not yet implemented. Ideally, multiple indirect validation methods are combined when assessing subject-specific model validity.

C. Study outline

The main goal of this study is to facilitate future OpenSim users with a scalable, fully consistent, generic upper-extremity model compatible with muscle-driven analyses, and a viable indirect validation method for subject-specific models. To achieve this goal, the thoracoscapular Delft shoulder and elbow model (TDSEM), a set of easy-to-use subject-specific scaling tools for the TSM and TDSEM, and an indirect validation method are developed in this study. These methods aim to raise the baseline of subject-specific scaling performance for upper-extremity models in OpenSim, reducing the chances of drawing incorrect conclusions in future studies. Data from the shoulder movement database (SMD) [65], [88] is used for evaluation.

Thoracoscapular Delft shoulder and elbow model: The TDSEM should be a closed-loop kinematic model containing the only fully-consistent, generic upper-extremity dataset [15], [16] available. To create this model, the closed-loop kinematic structure of the TSM and bony-landmark data from the DSEM are integrated into the model published as part of the dynamic arm simulator (DAS) project [20]–[22] containing the fully-consistent dataset. This model is not identical to the DSEM. Throughout this study, the performance of this model is compared to the performance of the TSM. Modelling efforts are deemed successful if marker errors after identical geometric scaling procedures are comparable between models, and results of muscle-driven simulations improve when using the TDSEM over the TSM.

Subject-specific scaling tools: A set of three easy-to-use scaling tools are developed for marker-based subject-specific scaling of both the generic TSM and TDSEM. The goal of these tools is to provide a baseline for subject-specific scaling performance for the TSM and TDSEM.

The model scaling tool optimizes geometric scaling based on marker-data provided. Performance is verified by evaluating inverse kinematic (IK) fit and comparing estimated-

to MRI-obtained lengths [65] of the clavicle, humerus, and radius in the subject’s modelled. Given the kinematic data used, average RMS marker error should not exceed 2cm in scaled models, and segmental length errors should not exceed 5% of their actual length.

The muscle-parameter optimization tool scales muscle-length properties to maintain the generic model’s normalized muscle-operating-range after geometric scaling and does not require additional data. This tool is a modified version of the algorithm by Modenese et al. [59]. Obtained optimization-fit should be better than, or comparable to other studies [18], [59], [60], and scaled parameters should compare to values in Penas [60] for the subjects modelled in both studies.

The muscle-volume scaling tool performs muscle-strength- and inertial scaling based on an estimation of total upper-extremity muscle-volume made using maximum isometric strength trials. This method is based on the uniform PCSA scaling approach by Bolsterlee et al. [65]. This scaling approach was derived from MRI data of the subjects modelled in this study. As such, this tool is not validated as the accuracy of muscle-volume estimates made is known.

Indirect validation method: The indirect validation method presented tries to implement the validation method suggested by Bolsterlee [5]. This method recreates the maximum isometric force trials in the SMD using an inverse dynamical (ID) static optimization (SO) procedure. Similar to the subjects during measurement, models can freely exert off-axis forces and torques: residuals. This procedure assumes that maximum directional force exertion during these trials is only limited by the strength of upper-extremity muscles. It is hypothesized that the lowest prescribed directional force resulting in SO-failure due to insufficient muscle-element strength matches the force-generating capacity of the subject at the hand if the model is sufficiently scaled. Thus, estimated maximum forces of subject-specific models created in this study are expected to be more similar to measured values than estimations obtained with a generic model. The desired accuracy of this method is for the error between estimated- and measured maximum directional forces to be of similar magnitude as the variability of the measured maximum force between attempts: about 10% of the maximum force. If successful, this method is another indirect validation tool for subject-specific models in the arsenal of future modellers. It should be used in conjunction with EMG- and kinematics-based indirect validation methods to draw a more informed conclusion about the validity of these models.

II. METHODS

This section describes the MSK modelling, scaling, and simulation methods used in this study. It elaborates the data adopted from the SMD in Section II-A, the generic MSK models in Section II-B, the normalized Hill-type muscle model in Section II-C, used subject-specific scaling methods in Section II-D, and the indirect validation method in Section II-E.

A. Modelled subjects

All data used in this study for subject-specific modelling is adopted from the SMD [65], [88]. All five subjects included in the SMD are modelled in this study.

Used kinematic data contains the location of bony landmarks in the global frame during motion trials. Their location is tracked using skin-fixed marker clusters on the thorax, scapula, humerus, and forearm. Their locations are indicated in Figure 1a. Locations of bony landmarks are tracked using their distance from one of these marker-clusters, obtained using palpation [89]. The SMD contains this data for two types of motion tasks: trials of upper-extremity RoM and activities of daily living (ADL). Accuracy hereof is thus limited by soft-tissue artifacts (STA), especially for the scapular marker-cluster [53], [90], [91]. During RoM- and ADL trials, EMG was recorded.

Force-transducer data adopted contains forces and torques measured at the handle during maximum isometric force trials. In these trials, subjects exerted maximum voluntary force in six directions – upwards, downwards, forwards, backwards, leftwards, and rightwards – whilst standing upright with 90° of elbow flexion. This experimental set-up is illustrated in Figure 1b. Each subject attempted this twice, without receiving feedback on force-magnitude. Kinematics were not recorded during these trials, as the force-transducer was outside of the range of the motion capture system. EMG is recorded during maximum isometric force trials.

B. Generic models

1) *Thoracoscapular shoulder model:* The TSM [14], [17] models motion of the human upper-extremity using six rigid-body segments and six joints connecting these segments. In this model, the thorax is considered a moving base. The location of all other segments with respect to the base is defined by 11 generalized coordinates; the model’s total degrees-of-freedom (DoF). The TSM contains 33 muscle-elements that cross the shoulder. Figure 2a is a visualization of the TSM.

The ST joint in the TSM constrains the center-point of the scapula to an ellipsoid surface attached to the thorax using two translational- and two rotational DoFs [17]. Figure 2b visualizes the ST joint. The SC joint is a universal joint modelled with two DoFs; axial rotation of the clavicle is constrained. The AC joint is a ball joint modelled as a point constraint; forcing a point on the scapula and clavicle to coincide. The glenohumeral (GH) joint is modelled as a gimbal joint with three DoFs, following ISB standard coordinates [92]. The humeroulnar (HU) joint is modelled as a hinge joint with one DoF. The radioulnar (RU) joint is modelled as a pivot joint with one DoF.

Segment dimensions and joint locations originate from Holzbaur et al. [93]. Inertial properties are adopted from the DSEM cadaver [15], [16].

Muscle-elements in the TSM are an aggregation of the muscle-bundles crossing the shoulder-girdle in the DSEM [71], [72]. Their paths are altered using wrapping sur-

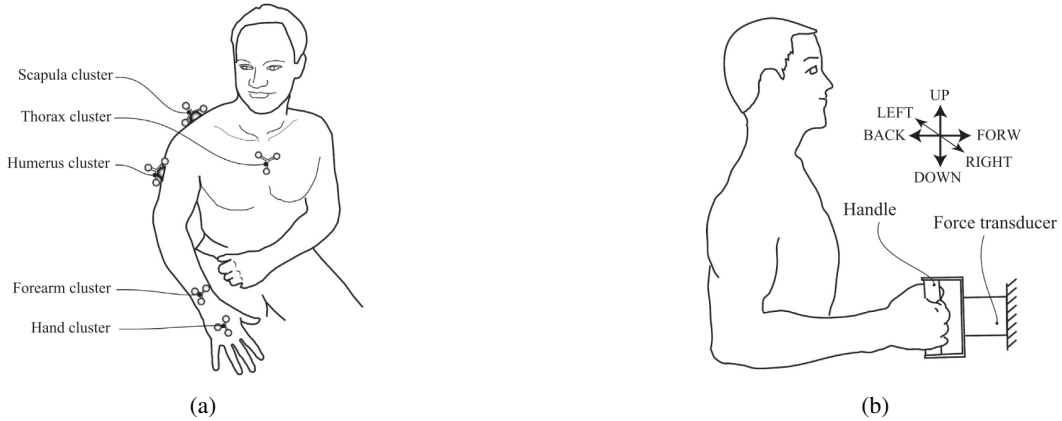


Fig. 1: **(a)**: The marker-cluster positioning used to collect the kinematic data presented in the shoulder movement database (SMD) [65], [88]. Bony landmark locations were tracked with respect to these clusters using their palpated [89] distance with respect to one of these clusters. **(b)**: Experimental set-up during maximum isometric force trials. Whilst standing upright with 90° of elbow flexion, subjects exerted maximum voluntary force in the six illustrated directions. Kinematics were not recorded during these trials. Force-transducer measurements during these trials are presented in the SMD. Figures are adopted from Bolsterlee et al. [65].

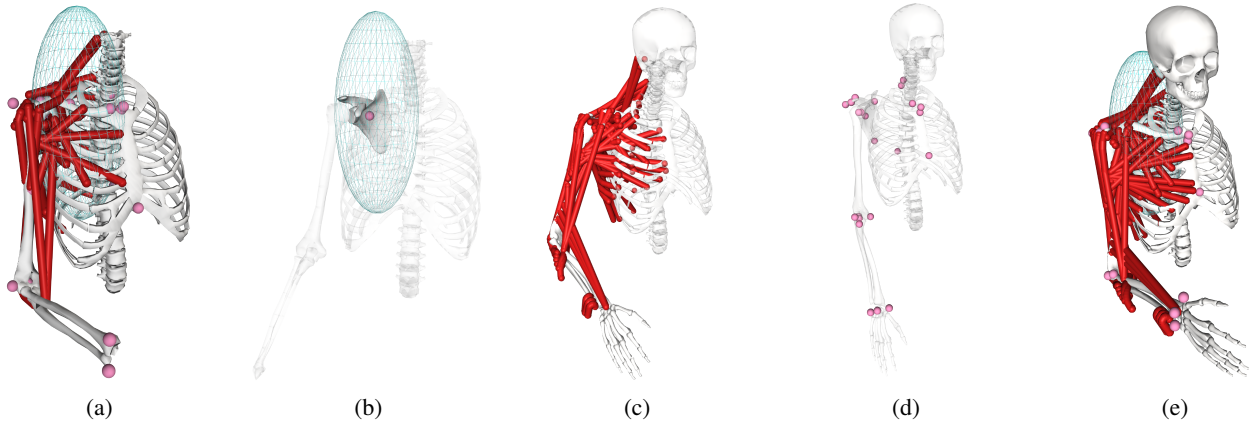


Fig. 2: **(a)**: The updated version of the generic thoracoscapular shoulder model (TSM) [14] used in this study. **(b)**: The scapulothoracic (ST) joint [17] – this joint constrains the center-point of the scapular body (indicated by the pink marker) to a thorax-fixed ellipsoid surface (the blue wire-frame) using four degrees-of-freedom (DoF). **(c)**: The OpenSim model present in the dynamic arm simulator (DAS) project's distribution [20]–[22]. **(d)**: The marker-set added to the DAS model from the Delft shoulder and elbow model's (DSEM) dataset [15], [16], [70]–[72]. **(e)**: The generic thoracoscapular Delft shoulder and elbow model (TDSEM) presented in this study – integrating the ST joint (Fig. (b)) and DSEM markers (Fig. (d)) into the DAS model (Fig (c)). All renders shown are captured in OpenSim 4.1 [6], [8]

faces, to comply with moment-arm boundaries from Ackland et al. [14], [94].

To this model, two alterations were made in this work: First, a cylindrical wrapping surface from the DSEM [16] was added to ensure that the muscle-element representing the *triceps brachii caput longum* produces an elbow-extension moment with a flexed elbow. Second, the default ranges of all generalized coordinates are adjusted based on the minimum and maximum values present in IK simulations of all RoM trials in the SMD – this greatly improves the performance of the muscle-length scaling algorithm (Section II-D.2).

2) Thoracoscapular Delft shoulder and elbow model:

The TDSEM integrates the previously described kinematic structure of the TSM into the OpenSim model from the DAS-project (Figure 2c) and adds bony-landmark data from the DSEM cadaver [15], [16] (Figure 2d). The TDSEM

contains 138 muscle-elements crossing the shoulder and elbow. Figure 2e is a visualization of the TDSEM.

To integrate the ST joint into the DAS model, the minor radii of the ellipsoid joint-surface were altered to the value of the minor radius of the ST contact surface in the DSEM [72]. This adjustment corrected for the difference in thoracic dimensions between both models. The SC joint in the TDSEM differs from the SC joint in the TSM and is modelled as a ball-joint, allowing axial rotation of the clavicle and adding one generalized coordinate. The TDSEM's pose is thus described with twelve DoFs. Similar to the TSM, default ranges of generalized coordinates are adjusted based on IK simulations of SMD RoM trials.

Segment dimensions, joint locations, and inertial properties of the TDSEM all originate from the DSEM cadaver [15], [16].

Muscle-element parameters and wrapping surfaces in the

TDSEM are unaltered from the DAS model, which are consistent with the DSEM cadaver [15], [16]. The computational Hill-type model of all muscle-elements is updated from the model by Schutte et al. [95] to the model by Millard et al. [96].

All palpated [89] marker-locations from the DSEM cadaver [15], [16] are added into the TDSEM by transforming their reported positions in the global coordinate frame to body-fixed coordinate frames. During this transformation, joint locations in the model coincided with palpated joint locations reported – IK RMSE was smaller than 2mm in this pose.

C. Normalized Hill-type muscle model

In OpenSim, muscles are modelled using the normalized Hill-type muscle model [57]. In Hill-type models, muscle fibers are represented using a contractile element (CE) modelling their force-generating capacity and a parallel elastic element (PE) modelling their elasticity. Tendons are modelled by a serial elastic element (SE), modelling their elasticity. The model schematically depicted in Figure 3a. Forces between the muscle fiber and tendon elements are always in equilibrium.

Normalized behavior of Hill-type muscle-elements is consistent between individuals [57]. This normalization requires five muscle-parameters: optimal fiber length l_o^m , tendon slack length l_s^t , maximum isometric contractile force F_{max}^m , maximum contractile velocity \dot{l}_{max}^m , and fiber pennation angle at optimal muscle-length α_o^m . Muscle force F^m is normalized \tilde{F}^m using F_{max}^m : Equation 1.

$$\tilde{F}^m = \frac{F^m}{F_{max}^m} \quad (1)$$

Muscle length l^m is normalized \tilde{l}^m using l_o^m : Equation 2.

$$\tilde{l}^m = \frac{l^m}{l_o^m} \quad (2)$$

Tendon length l^t is normalized \tilde{l}^t using l_s^t and can also be described using tendon strain ϵ^t : Equation 3.

$$\tilde{l}^t = \frac{l^t}{l_s^t} = 1 + \epsilon^t \quad (3)$$

Contraction velocity \dot{l}^m is normalized $\tilde{\dot{l}}^m$ using \dot{l}_{max}^m : Equation 4.

$$\tilde{\dot{l}}^m = \frac{\dot{l}^m}{\dot{l}_{max}^m} \quad (4)$$

Pennation angle α^m at any muscle-length is calculated using l_o^m , l^m , and α_o^m : Equation 5.

$$\alpha^m = \text{asin} \left(\frac{l_o^m \cdot \sin(\alpha_o^m)}{l^m} \right) \quad (5)$$

Figure 3b graphs the normalized force-length relations of the muscle-model.

D. Subject-specific scaling tools

Subject-specific scaling in this study is performed with three scaling tools written in MATLAB [97] using the API of OpenSim 4.1. The *model scaling tool* performs geometric scaling by optimizing segmental scale-factors such that IK error is minimized. The *muscle-parameter optimization tool* performs muscle-length scaling such that the normalized operating range of muscle-elements is maintained after geometric scaling. The *muscle-volume scaling tool* performs muscle-strength and inertial scaling based on a uniform muscle-volume scale-factor estimated with a measure of the subject's mean maximum isometric force exertion. For use of these scaling tools, the previously described order is required.

1) *Geometric scaling*: Inputs for the model scaling tool are a generic model – either the TSM or TDSEM – and marker-data from a (set of) kinematic trial(s). The output of the tool is a geometrically scaled version of the generic model chosen.

For this study, scaled versions of both the TSM and TDSEM are made for all 5 subjects in the SMD using the model scaling tool. RoM trials recorded wherein a minimal number of marker-frames were missing are used as input – the IK-tool requires thoracic bony landmarks to be defined (not NaN) at all evaluated time-steps, leading to the linear interpolation of missing frames in the small number of instances where this was required. Frames of all trials are combined and down-sampled at 1 seconds intervals. This down-sampling greatly decreases optimization time and is recommended. The interval is chosen such that the entire range of poses attained by the subject is included.

The total squared marker error of OpenSim's IK-tool is evaluated using the markers representing bony-landmarks on the thorax, scapula, humerus, radius, and ulna. Clavicular bony-landmarks were ignored, as kinematic data in the SMD did not include a skin-fixed marker-cluster on the clavicle. The virtual markers – like the one tracking the GH-joint *in vivo* [98], [99] commonly calculated during marker trials – can also be included, but were not used in this study.

Thorax and scapula are scaled using three separate scale factors along these segment's body-fixed axes. The radii of the ST joint and its location in the thorax are scaled with the thoracic scale-factors. Long segments; the clavicle, humerus, and forearm are scaled using a single, uniform factor – radius and ulna share a scale-factor. The tool uses MATLAB's *fminsearch* algorithm to find the set of these scale factors that produces the minimum total squared marker error in an IK-trial.

The model scaling tool allows for a further, separate, optimization of ST joint parameters: its ellipsoid radii and location and orientation in the thorax and scapula. This was not performed for scaled models in this study, as further reductions of total errors were marginal. In case the movement studied involves significant spinal bending or twisting, optimization of these parameters can further improve kinematic fit [17].

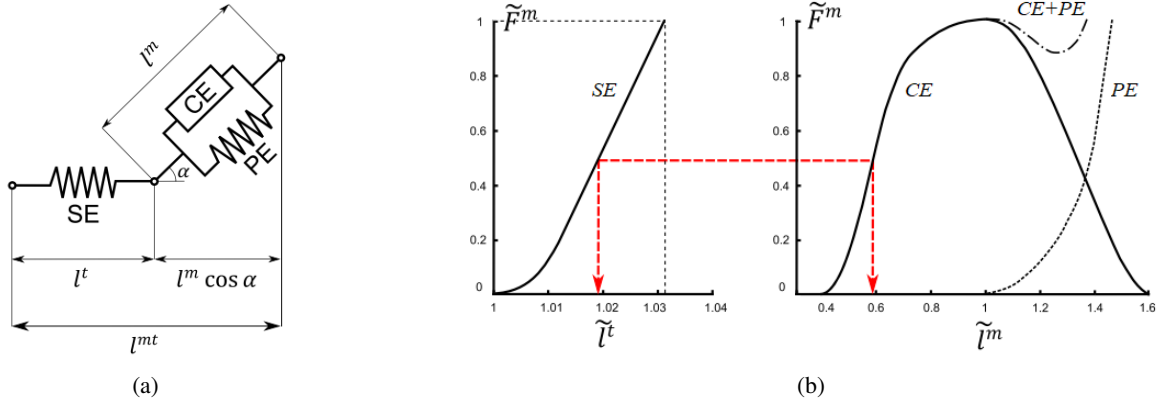


Fig. 3: (a): Schematic depiction of the Hill-type muscle model, consisting of a contractile element (CE) and parallel elastic element (PE) representing a muscle body, and a serial elastic element (SE) representing a tendon. Forces transferred between these elements are always in equilibrium (b): Curves illustrating the normalized behavior of a Hill-type muscle-tendon unit with a pennation angle at optimal muscle length (α_o^m) of 0. The curves relate the maximum normalized force \tilde{F}^m of the muscle-tendon unit to normalized tendon length \tilde{l}^t (left) and normalized muscle-fiber length \tilde{l}^m (right). In the left-sided plot: the solid line indicates passive tendon-force of the SE and the dashed lines indicate maximum tendon elongation: $\tilde{l}^t=1.033$. In the right-sided plot: the solid line indicates the maximum active fiber-force of the CE, the dashed line indicates the passive fiber-force of the PE, and the dashed-dotted line indicates their sum. The red dashed line illustrates an equilibrium between muscle- fiber and tendon elements during a maximum isometric contraction. Figures are adopted from Modenese et al. [59].

2) *Muscle-length scaling*: Inputs for the muscle-parameter optimization tool are a generic model and a geometrically scaled version of that generic model. The output of the tool is a version of the geometrically scaled model with optimized optimal fiber- and tendon slack length properties. The tool is a modified version of the algorithm presented by Modenese et al. [59]. Alterations include:

- Partial updating of the original tool to function with the latest structure of model-files introduced in OpenSim 4.0 [8].
- Added functionality for proper functioning with the closed-loop kinematic structure of the TSM and TD-SEM, and muscle-elements representing the *serratus anterior* which' tendon slack length is zero. This property is maintained in optimization.
- Introduction of a limit-value for the total number of model-poses sampled in optimization, reducing the number of equally spaced evaluations made per DoF until this limit is no longer exceeded. This is required for the muscle-parameter optimization tool to function on most desktop processors.
- Inclusion of the option to select alternate solving algorithms for the least-squares optimization performed by the tool. The original algorithm produces unfeasible optimized parameters for muscle-elements crossing the ST joint, predicting up to a 2500% increase of tendon slack length from the generic to the scaled model.

The length of a muscle-tendon-unit l^{mt} for any model-pose is given by it's pennation angle α^m , normalized-muscle- \tilde{l}^m and tendon \tilde{l}^t lengths at any instance, given the muscle's optimal fiber length l_o^m and tendon slack length l_s^t properties: Equation 6.

$$l^{mt} = \{\tilde{l}^m \cdot \cos(\alpha^m)\}l_o^m + \tilde{l}^t \cdot l_s^t \quad (6)$$

The algorithm samples α^m , \tilde{l}^m , and \tilde{l}^t during an equilibrated maximum isometric contraction of the muscle in the generic model (subscript gen in Equation 9), and l^{mt} in the scaled model (subscript sc in Equation 9), in poses with identical generalized coordinate values. The total number of poses sampled per muscle n^m is chosen such that the operating range is sufficiently sampled. n^m depends on the number of equally spaced sampled per generalized coordinate N_{ev} and the number of generalized coordinates separating the muscle's origin and insertion points N_q^m : Equation 7.

$$n^m = (N_{ev})^{N_q^m} \quad (7)$$

Modenese et al. [59] determined with a lower-extremity model, that $N_{ev} \geq 10$ was required for convergent optimization results. In this work, a limit-value for n^m is introduced: n_{lim} . n_{lim} leads to a variable N_{ev} between muscles in a model. This addition is required for upper-extremity muscles as $N_q^m \leq 7$, due to the increased mobility compared to lower-extremity models used previously. This increased mobility results in a sufficient sampling of operating range for lower values of N_{ev} . Thus, for all optimization procedures discussed in this work $N_{ev} \leq 10$. Without this introduction, the algorithm also cannot be performed with upper-extremity models using most current desktop processors due to exponentially increasing array sizes. Thus, N_{ev} is decreased until n_{lim} is no longer exceeded by n^m : Equation 8.

$$\text{while } n^m > n_{lim}, \quad N_{ev} = N_{ev} - 1 \quad (8)$$

The effect of selected n_{lim} -value on optimization convergence and optimization time is described in Section III-B.

Using all sampled poses within the generic muscle's normalized operating range $-0.5 \leq \tilde{l}^m \leq 1.5$ and $\alpha^m \leq 84^\circ$

– the linear system in Equation 9 is constructed [59].

$$\begin{bmatrix} l_1^{mt} \\ l_2^{mt} \\ \vdots \\ l_n^{mt} \end{bmatrix}_{sc} = \begin{bmatrix} \tilde{l}_1^m \cdot \cos(\alpha_1^m) & \tilde{l}_1^t \\ \tilde{l}_2^m \cdot \cos(\alpha_2^m) & \tilde{l}_2^t \\ \vdots & \vdots \\ \tilde{l}_n^m \cdot \cos(\alpha_n^m) & \tilde{l}_n^t \end{bmatrix}_{gen} \begin{bmatrix} l_o^m \\ l_s^t \end{bmatrix}_{sc} \quad (9)$$

This linear system is solved for the values of l_o^m and l_s^t using a pseudo-inverse. In Modenese's [59] tool, this solution was recomputed using a two-step approach if the optimized $l_s^t \leq 0$. The two-step approach first optimizes l_o^m whilst l_s^t is temporarily fixed to it's proportion in the generic model, and then computes l_s^t given the optimized l_o^m . In this work, functionality is added for the exclusive use of this two-step scaling approach, as the default least-squares solution does not yield physiologically plausible values for muscles crossing the ST joint.

3) *Muscle-strength scaling*: Input for the muscle-volume scaling tool is the generic model, the geometrically scaled version of this model with scaled muscle-length-parameters, and the mean maximum force measured for the subject during their maximum isometric force trial. The output of the tool is the scaled model with scaled muscle-strength- and inertia.

A muscle-element's maximum isometric contractile force F_{max}^m is calculated with the muscle's physiological cross-sectional area $PCSA^m$ and the maximum stress of muscle-tissue σ_{max} : Equation 10.

$$F_{max}^m = PCSA^m \cdot \sigma_{max} \quad (10)$$

$PCSA^m$ is defined by muscle-volume v^m , pennation angle at optimal muscle length α_o^m , and optimal fiber length l_o^m : Equation 11 [100].

$$PCSA^m = \frac{v^m \cdot \cos(\alpha_o^m)}{l_o^m} \quad (11)$$

Bolsterlee et al. [65] found a value of $\sigma_{max}^{sc} = 69.4 \frac{N}{cm^2}$ for uniformly-scaled upper-extremity muscles, instead of the value ($\sigma_{max}^{gen} = 100 \frac{N}{cm^2}$) used to obtain the generic-model's F_{max}^m -parameters. This the scaling-algorithm corrects this difference.

First, the subject's total upper-extremity muscle volume v_{tot}^s is estimated using it's correlation [65] with a subject's mean maximum isometrically exerted force \bar{F}_{max}^s : Equation 12.

$$v_{tot}^s = f(\bar{F}_{max}^s) \quad (r = 0.97) \quad (12)$$

Second, scale-factor s_v is calculated using v_{tot}^s and the total upper-extremity muscle volume of the cadaveric specimen v_{tot}^{gen} : Equation 13.

$$s_v = \frac{v_{tot}^s}{v_{tot}^{gen}} \quad (13)$$

Third, muscle-element volume in the generic model $v^{m,gen}$ is calculated with generic muscle-parameters: Equation 14.

$$v^{m,gen} = \frac{F_{max}^{m,gen} \cdot l_o^{m,gen}}{\cos(\alpha_o^m) \cdot \sigma_{max}^{gen}} \quad (14)$$

Fourth, $v^{m,gen}$ is scaled with s_v : Equation 15.

$$v^{m,sc} = s_v \cdot v^{m,gen} \quad (15)$$

Last, the scaled value of F_{max}^m ($F_{max}^{m,sc}$), is calculated with scaled-model muscle-parameters: Equation 16.

$$F_{max}^{m,sc} = \frac{v^{m,sc} \cdot \cos(\alpha_o^m)}{l_o^{m,sc}} \cdot \sigma_{max}^{sc} \quad (16)$$

4) *Inertial scaling*: Segmental inertias are scaled using scale-factor s_v , see Section II-D.3. Segment mass – translational inertia – in the scaled model $m^{b,sc}$ is the segment mass in the generic model $m^{b,gen}$ scaled with s_v : Equation 17.

$$m^{b,sc} = s_v \cdot m^{b,gen} \quad (17)$$

Segment rotational inertia in the scaled model $I^{b,sc}$ is the segment inertia in the generic model $I^{b,gen}$ scaled with s_v : Equation 18.

$$I^{b,sc} = s_v \cdot I^{b,gen} \quad (18)$$

E. Indirect validation method

1) *Static optimization procedure*: SO uses an ID approach to find an actuator-activation ($\mathbf{a}^m, \mathbf{a}^r$) set satisfying the MSK model's system equation (Equation 19), ignoring muscle-excitation- and tendon-dynamics. This solution is constrained by prescribed model-states (\mathbf{q}) – describing the model's pose with generalized coordinates – and their derivatives ($\mathbf{q}, \dot{\mathbf{q}}$), and prescribed generalized external forces $\boldsymbol{\tau}_{ext}$. The generalized system equation of a MSK model at any instance given by it's mass matrix $\mathbf{M}(\mathbf{q})$, Coriolis and centrifugal force vector $\mathbf{C}(\mathbf{q}, \dot{\mathbf{q}})$, gravitational force vector $\mathbf{G}(\mathbf{q})$, generalized muscle-forces $\boldsymbol{\tau}_m$, $\boldsymbol{\tau}_{ext}$, and generalized residual- and reserve force vector $\boldsymbol{\tau}_r$: Equation 19 [6].

$$\mathbf{M}(\mathbf{q}) \cdot \ddot{\mathbf{q}} + \mathbf{C}(\mathbf{q}, \dot{\mathbf{q}}) + \mathbf{G}(\mathbf{q}) = \boldsymbol{\tau}_m + \boldsymbol{\tau}_r + \boldsymbol{\tau}_{ext} \quad (19)$$

Generalized forces exerted by all muscle-elements $\boldsymbol{\tau}_m$ depend on each muscle-elements activation (a^m), state-dependent force-generating capacity $f(l^m(\mathbf{q}), \dot{l}^m(\mathbf{q}, \dot{\mathbf{q}}), F_{max}^m)$, and moment arm about each generalized coordinate \mathbf{r}^m : Equation 20.

$$\boldsymbol{\tau}_m = \sum_{m=1}^{N_m} \{a^m \cdot f(l^m(\mathbf{q}), \dot{l}^m(\mathbf{q}, \dot{\mathbf{q}}), F_{max}^m)\} \mathbf{r}^m \quad \text{with } 0 \leq a^m \leq 1 \quad (20)$$

Residual- and reserve actuators are additional, fictional actuators added into a MSK model to account for modelling errors that can otherwise result in failed optimization steps. Residual actuators are added between the MSK model and the external world to account for reaction forces not- or incorrectly prescribed in $\boldsymbol{\tau}_{ext}$. Reserve actuators are added to a model's joints to account for instances where muscle-elements cannot generate forces required to perform the prescribed motion. Their generalized contributions $\boldsymbol{\tau}_r$ are given by each actuator's activation a^r , optimal value F_{opt}^r ,

and moment arm about each generalized coordinate r^r : Equation 21.

$$\tau_r = \sum_{r=1}^{N_r} \{a^r \cdot F_{opt}^r\} r^r \quad \text{with } -\infty \leq a^r \leq \infty \quad (21)$$

Generalized forces exerted by all prescribed external loads τ_{ext} are given by external force-vector F_{ext}^f and it's moment arm about each generalized coordinate r^f , and external torque-vector T_{ext}^t and it's component acting along each generalized coordinate r^t : Equation 22.

$$\tau_{ext} = \sum_{f=1}^{N_f} \{F_{ext}^f \cdot r^f\} + \sum_{t=1}^{N_t} \{T_{ext}^t \cdot r^t\} \quad (22)$$

As MSK models contain more actuators than generalized coordinates, most load conditions can be satisfied by a near-infinite amount of actuator-activation combinations. As such, actuator-activation values are determined by optimizing objective function J , whilst satisfying Equation 19. OpenSim's native objective function minimizes the squared activity of all actuators for each evaluated instance: Equation 23.

$$J = \sum_{m=1}^{N_m} (a^m)^2 + \sum_{r=1}^{N_r} (a^r)^2 \quad (23)$$

2) *Method implementation*: The TSM- and TDSEM generic models (Section II-B) and scaled versions hereof – scaled to resemble all five subjects in the SMD using the methods described in Section II-D – are used with this simulation method. The indirect validation method was thus performed with twelve separate models.

During static optimization, each model is constrained to a static pose ($\mathbf{q}, \dot{\mathbf{q}} = 0$), following identical instructions as the subject did during their maximum isometric force measurements, see Figure 1b. Figures 2a and 2e are highly similar to the static poses of all models. As kinematics were not recorded by Bolsterlee et al. [65] during these measurements, the model poses used are an approximation of actual subject-poses.

Six different external loads are applied to each model in separate simulations. The point of application of all external loads is at the origin of the hand's coordinate frame; the location of the radiocarpal joint in both models. The external loads contain a uni-directional force-vector ranging from 1 to 400N in 1N intervals – measured maximal forces ranged from 46.7 to 366.5N [65]. The direction of this force is opposite to the intended direction of force exertion. This way, the model is required to exert force in the direction of interest to maintain its prescribed static pose. No external torques are prescribed in any simulation.

During the maximum force measurements, subjects were free to exert residual forces in directions other than the one maximized, and residual torques. To allow each model the same freedom in simulation, residual actuators are added to the model at the point where external loads are applied. Two residual actuators exerting force – in both residual

directions – and three residual actuators exerting torque – along all three main axes – are added in each simulation. Their optimal values were chosen as 1000N and 1000Nm respectively, to minimize their influence on optimization results. Further increasing these values did not significantly influence optimization results.

In the case of simulations involving the generic- and scaled versions of the TSM, two reserve actuators are also added. These reserves are added to the elbow flexion and forearm pronation coordinates because most muscles crossing these joints are not included in the TSM. Their optimal values were arbitrarily chosen as 20Nm and were consistent for both the generic- and scaled versions of the TSM.

In the case of simulations involving the generic- and scaled versions of the TDSEM, the coordinate describing clavicular axial rotation is fully constrained during simulations. As the TDSEM does not contain an element modelling the conoid ligament, this was required for muscle-elements attaching to the clavicle to freely exert force. In the TSM, this DoF is not present.

III. RESULTS

This section denotes the results of geometric scaling in Section III-A, muscle-length scaling in Section III-B, muscle-strength scaling in Section III-C, inertial scaling in Section III-D, and the indirect validation method in Section III-E.

A. Geometric scaling

Geometric scaling of the TSM and TDSEM generic models is performed for all five subjects in the SMD. Methods are elaborated in Section II-D.1. Optimization times on an i7-7700HQ processor range from 40 to 120 minutes. Duration linearly depends on the number of sampled frames used in optimization.

The final RMS marker error of the scaling procedure is reported per subject and model in the top two rows of Table I. On average, the RMS marker error of the scaling procedure between the TSM and TDSEM is similar. Overall, optimization fit is limited by the accuracy of marker-data provided. Accuracy of the marker-cluster data used is limited STA's [53]. STA's cause large tracking errors for the scapula and humerus [90], [91]. For future scaling procedures using similar data, an optimization RMS marker error ≤ 2 cm is thus achievable.

Geometric scaling is verified using independent kinematic data not used in the scaling procedure. This data is an ADL-trials from the SMD. For subjects 1 and 2, this is a hair-combing motion. For subjects 3, 4, and 5, this is a motion of perineal care. The middle four rows of Table I contain the RMS marker error of the generic- and scaled versions of the TSM and TDSEM for each subject. These values are obtained using OpenSim's IK-tool. The desired kinematic fit of ≤ 2 cm is achieved by most scaled models, but never with the generic model. The percentual change in RMS marker error between generic- and scaled versions of the TSM and TDSEM are given in the bottom two rows. For all subjects,

	Subject 1	Subject 2	Subject 3	Subject 4	Subject 5	Average
TSM: Scale optimization RMS marker error [cm]	1.7	1.5	1.8	1.8	2.1	1.8
TDSEM: Scale optimization RMS marker error [cm]	2.0	2.1	1.8	1.8	2.0	1.9
Generic TSM: IK RMS marker error [cm]	3.4	2.8	2.6	2.6	3.2	2.9
Generic TDSEM: IK RMS marker error [cm]	3.2	3.1	2.1	2.3	2.2	2.6
Scaled TSM: IK RMS marker error [cm]	1.8	1.6	2.1	1.9	2.5	2.0
Scaled TDSEM: IK RMS marker error [cm]	2.3	2.5	2.0	1.8	2.0	2.1
TSM: change in RMS marker error [%]	-47	-43	-19	-27	-22	-31
TDSEM: change in RMS marker error [%]	-28	-19	-5	-22	-9	-19

TABLE I: Table containing metrics used to evaluate geometric scaling. Scaled versions of the thoracoscaphular shoulder model (TSM) and thoracoscaphular Delft shoulder and elbow model (TDSEM) (Section II-B) are created for all five subjects in the shoulder movement database (SMD) (Section II-A). Scaling is optimized based on multiple motion-trials in which the subjects’ upper-extremity range-of-motion (RoM) was tested. Inverse-kinematic (IK) root-mean-square (RMS) marker error of the final optimized model is reported in the top two rows. The middle four rows pertain RMS marker errors from OpenSim’s IK tool when modelling an independent motion trial not used in optimization. The bottom two rows denote the percentual change in RMS marker error between the generic- and scaled versions of both models.

RMS error decreases when using scaled models. On average, RMS error magnitudes of TSM-based and TDSEM-based scaled models are comparable. A larger percentual decrease in RMS error is observed for TSM-based models due to the worse kinematic fit of the generic model for most subjects.

For scaled versions of the TDSEM, scale-factors of long segments – clavicle, humerus, and forearm – can be validated using segment-length-ratios between subject- and cadaveric MRI-data [65]. On average, clavicle length is overestimated $4.4 \pm 8.2\%$ or $5.99 \pm 11.75\text{mm}$. Note that no clavicular markers are used in the scaling procedure. On average, humerus length is overestimated $4.3 \pm 2.1\%$ or $14.17 \pm 7.48\text{mm}$. On average, radius length is underestimated $1.3 \pm 4.6\%$ or $3.81 \pm 11.81\text{mm}$. Note that the radius the model is scaled using a scale-factor shared with the ulna. For most, but not all, scaled segments, the desired accuracy of 5% is thus achieved.

B. Muscle-length scaling

1) *Effect of limit-parameter and scaling algorithm:* The effect of the introduced evaluated-poses-limit parameter is evaluated using the default scaling algorithm by Modenese et al. [59] (Figure 4a) and using the two-step scaling algorithm exclusively (Figure 4b). These results are obtained using two scaled versions of the TSM: representing subjects 3 and 5 in the SMD. Optimization times of muscle-elements are comparable for both scaling algorithms and depend on: 1. the number of DoFs crossed by muscle-element origin and insertion, and 2. used limit value – increasing until ten evaluations per crossed coordinates are made.

Regardless of the scaling algorithm, optimized optimal fiber length and tendon slack length values quickly converge for muscle-elements not crossing the ST joint. For muscle-elements crossing the ST joint – indicated by blue and pink data in Figure 4 – optimized optimal fiber length and tendon slack length values are highly variable when using the default scaling algorithm. Furthermore, the default algorithm results in scaled tendon slack length values for these muscles not physiologically plausible [18], [101] – predicting up to a 2500% increase of tendon slack length from the generic

values. Exclusive use of the two-step algorithm resulted in far more convergent and physiologically plausible scaled values. Within the sampled range of limit-values, RMS optimization error did not converge for muscles crossing the ST joint. Yet, the RMS optimization error for these muscles is very low for all limit values evaluated.

2) *Muscle-length scaling results:* For muscle-length scaling of TSM-based scaled models, a limit value of 100,000 poses is used. For TDSEM-based scaled models, a limit value of 20,000 poses is used. This decrease in poses is required for successful optimization due to the increased number of muscle-elements in the TDSEM. Using an i7-7700HQ processor, scaling a TSM-based model takes about 120 minutes, and scaling a TDSEM-based model about 150 minutes.

Results of muscle-length scaling of the TSM- and TDSEM-based model for all five subjects in the SMD are denoted in Table II. Differences in average change between models are because the generic TSM is smaller and has fewer muscle-elements than the generic TDSEM. For both models, scaled optimal fiber length and tendon slack length values do not linearly correspond to scale-factors from geometric scaling.

The optimization fit (RMSE) of TSM-based models is comparable values reported in other works [18], [59], [60]. The optimization fit of TDSEM-based models is, on average, better. This likely results from the inclusion of muscles crossing the elbow, which’ optimal fiber length and tendon slack length is estimated using a low number of poses – 10 or 100 – resulting in a lower RMSE.

Optimization results of TDSEM-based models for subjects 3 and 5 can be compared to the results of Peñas [60]. Peñas used scaled versions – geometric scaling method differed – of the DSEM representing both subjects. Results from this study largely agree with results by Peñas. Changes in optimal fiber length- and tendon slack length change are similar, though different in magnitude. These differences are small (<5%) and originate from the difference in the geometric scaling method.

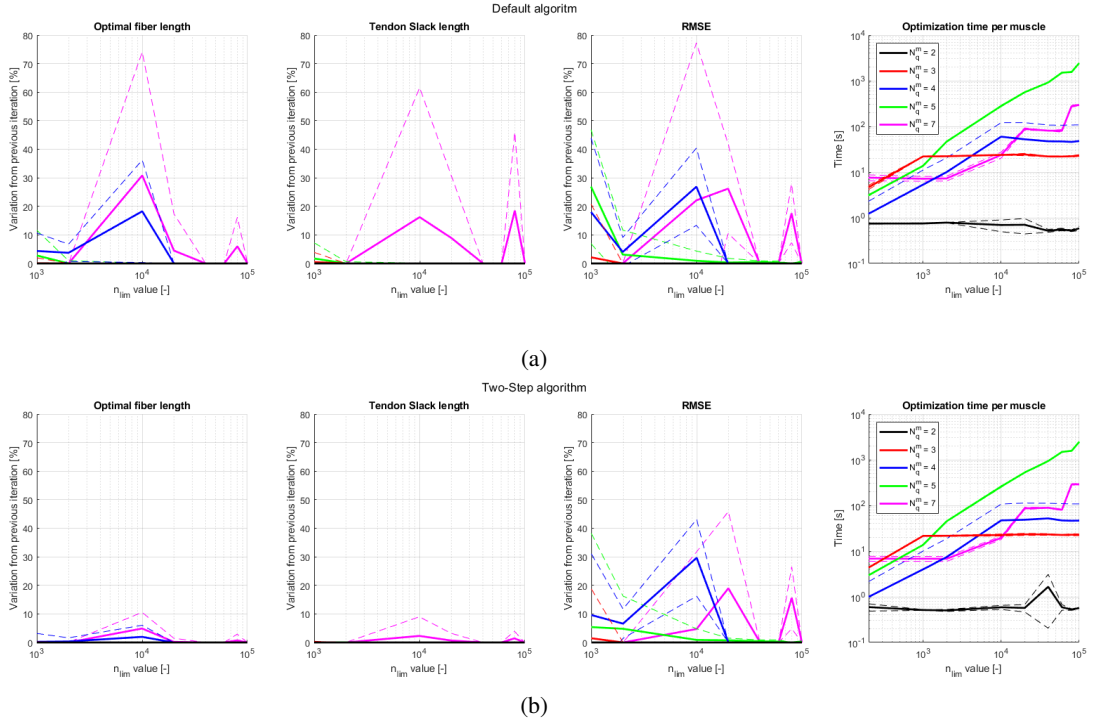


Fig. 4: Plots illustrating the convergence of muscle-length scaling results as a function of the introduced evaluated-poses-limit-parameter n_{lim} . **(a)**: Optimization performance using default scaling algorithm by Modenese et al. [59]. **(b)**: Optimization performance exclusively using a two-step scaling algorithm. Data shown is obtained from optimization of two scaled versions of the thoracoscapular shoulder model (TSM), representing subjects 3 and 5 in the Shoulder Movement Database. Line color indicates the number of degrees-of-freedom between muscle- origin and insertion in the TSM N_q^m . Solid lines represent the mean over all muscles in both models sharing the same N_q^m -value. Dashed lines indicate one standard-deviation from this mean.

	Subject 1	Subject 2	Subject 3	Subject 4	Subject 5	Average
TSM: l_o^m change [%]	+12.6 ± 6.5	-16.4 ± 4.3	-4.4 ± 4.9	+11.6 ± 5.1	+0.6 ± 6.0	-
TDSEM: l_o^m change [%]	+6.0 ± 5.8	-2.6 ± 5.5	-1.9 ± 5.8	+2.6 ± 5.7	+0.1 ± 5.6	-
TSM: l_s^t change [%]	+18.4 ± 7.1	-11.6 ± 5.7	+0.5 ± 5.8	+22.2 ± 6.3	+5.7 ± 5.8	-
TDSEM: l_s^t change [%]	+9.6 ± 6.0	-2.6 ± 5.0	+0.3 ± 5.0	+2.2 ± 5.6	+0.0 ± 5.2	-
TSM: Optimization RMSE [cm]	1.19 ± 0.80	1.09 ± 0.87	1.08 ± 1.06	1.65 ± 1.42	1.09 ± 1.12	1.22 ± 1.05
TDSEM: Optimization RMSE [cm]	1.02 ± 0.93	0.36 ± 0.41	0.53 ± 0.63	0.44 ± 0.44	0.35 ± 0.45	0.54 ± 0.57

TABLE II: Table denoting change in optimal fiber length l_o^m and tendon slack length l_s^t per subject from their generic values: the result of muscle-length scaling. This was performed with scaled versions of the thoracoscapular shoulder model (TSM) and thoracoscapular Delft shoulder and elbow model (TDSEM) for all subjects in the shoulder movement database. Root-mean-square-error (RMSE) values indicate optimization fit. Values reported are the mean and standard deviation taken over all muscle-elements in a model.

	Subject 1	Subject 2	Subject 3	Subject 4	Subject 5	Average
Scale factor s_v	1.53	0.87	1.11	2.03	1.81	-
TSM: F_{max}^m change [%]	-4.7 ± 8.1	-26.8 ± 9.9	-18.5 ± 10.5	+30.2 ± 28.1	+12.2 ± 9.5	-
TDSEM: F_{max}^m change [%]	+1.5 ± 9.9	-38.2 ± 2.2	-21.3 ± 4.4	+37.6 ± 8.7	+25.6 ± 6.3	-

TABLE III: Table denoting changes resulting from muscle-strength scaling. Scaling is performed with scaled versions of both the thoracoscapular shoulder model (TSM) and thoracoscapular Delft shoulder and elbow model (TDSEM). Reported changes in maximum isometric muscle force F_{max}^m are with respect to the value in the generic model. Values reported are the mean and standard deviation taken over all muscle-elements in a model.

C. Muscle-strength scaling

Muscle-strength scaling is performed with scaled versions of the TSM- and TDSEM generic model for all five subjects in the SMD. Resulting changes in average maximum isometric muscle-element strength, and scale-factors used

herefore, are tabulated in Table III. The duration of this scaling procedure is less than five seconds.

Maximum isometric muscle-element strength cannot be validated directly. However, the accuracy of muscle-volume estimates obtained using the subject-specific scale-factor is known. This accuracy is presented in Bolsterlee et al. [65]

and compared to MRI measurements of muscle-volume for the same set of subjects.

D. Inertial scaling

Inertial scaling is performed with scaled versions of the TSM- and TDSEM generic model for all five subjects in the SMD using the volumetric scale-factor in Table III. No measures of segmental inertia are presented in the SMD. Values estimated by scaling can thus not be directly validated.

When evaluating instances of measured maximum isometric force exertion using SO, generalized forces – obtained with OpenSim’s ID-tool – changed less than 0.1% as a result of inertial scaling. The effect of inertial scaling is thus negligible for the muscle-driven simulations of the maximum isometric force trials.

E. Indirect validation method

For the TDSEM, static optimization failure due to insufficient muscle-element strength happened for forward- and backward force exertion with scaled models of subjects 2 and 3, and for rightward force exertion with scaled models of subjects 1, 2, and 3. For all other models and directions, static optimization failure did not occur in the tested range of directional forces: 1 to 400N. Static optimization failure occurs at equal levels of muscle-activation for all TDSEM-based models. At this activation level, all muscle-elements capable of exerting force in the intended direction are fully contracting. Figure 5 illustrates results for forward force exertion. These results are comparable to other tested directions of force for TDSEM-based models. Estimations of maximum isometric force exertion that can be made using the posed method are 50- to 400% larger than measured maximum forces. Averaged over all directions, the measured between-subject proportionality of mean maximum directional forces is introduced in the scaled models. This is the result of performed muscle-strength scaling. Measured between-subject proportionality in individual directions is introduced, as observed in Figure 5.

For the TSM, no static optimization failure due to insufficient muscle-element strength occurred in any direction for any model in the tested range of directional force: 1 to 400N. As such, no estimations are made using TSM-based models. The lack of observed static optimization failure is the result of the required reserve actuator inclusion in these models. Reserve actuator torques are not limited, causing static optimization failure not to occur as a result of insufficient strength in muscles crossing the elbow flexion and forearm pronation DoFs. Measured between-subjects proportionality of maximum strength is not observed in TSM-based models; neither in individual directions or on average.

In general, the indirect validation method performs better with TDSEM-based models than TSM-based models, as measured between-subject strength proportions are – on average – observed in TDSEM-based models only. Yet, estimations of maximum force are too dissimilar from measured values for all models. Any (in-)validating conclusions about an individual subject-specifically scaled model cannot be

made using this method. The desired degree of accuracy for this method is not reached.

IV. DISCUSSION

This section discusses the TDSEM in Section IV-A, the subject-specific scaling tools in Section IV-B, the indirect validation method in Section IV-C, and recommended future improvements in Section IV-D.

A. Thoracoscapular Delt shoulder and elbow model

On average, the kinematic fit of TDSEM-based- and TSM-based subject-specific models are comparable. The kinematic fit attainable with both models is likely limited by STAs present in the used marker-data [53], [90], [91]. This suggests that the goal set for the desired kinematic accuracy of the TDSEM is reached.

It is found that muscle-element attachments and wrapping geometries in the forearm presented in Nikooyan et al. [16] are incorrectly implemented in the DAS model. Muscle-elements of the DAS model are directly adopted in the TDSEM. An example hereof is the insertion of the brachioradialis’ muscle-elements on the radius: The distance between the insertion site and the radial styloid location differs 2.86cm between the DAS model and the DSEM. The distance between origin sites and the lateral epicondyle location differs 0.14cm between the DAS model and DSEM. Whilst the latter difference can be attributed to errors made in the process of adding marker-data in this study, the former difference is too large to be fully caused hereby. Similar observations are made for other muscle-elements attaching to the radius. Furthermore, the wrapping cylinders representing the radius are not oriented in the same direction as in the DSEM, and joint-locations are not identical between models. Discontinuous muscle-lengths are observed in some IK trials as a result of these differences. This needs to be addressed before the TDSEM can be distributed, as it invalidates the muscle-elements in the forearm. This is best done by reconstructing the model from DSEM source files.

All muscle-driven simulations described in this study pertain to the indirect validation method presented. In these simulations, results obtained with TDSEM-based models are more in line with expectations than TSM-based model results: Measured between-subject proportionality in strength exertion is better observed in TDSEM-based subject-specific models. This resulted from the inclusion of all musculature in the arm in the TDSEM, regardless of errors herein. As such, future muscle-driven simulation results obtained with TDSEM are expected to be an improvement over results obtained with the TSM. Muscle-driven simulations with the TDSEM are more computationally expensive than with the TSM. The type of task studied should thus be considered when selecting which of the two generic upper-extremity models is used.

The TDSEM is not an OpenSim implementation of the DSEM. Besides the differences in muscle-element attachments and wrapping geometries in the forearm mentioned previously, there are further differences: First, the ST joint

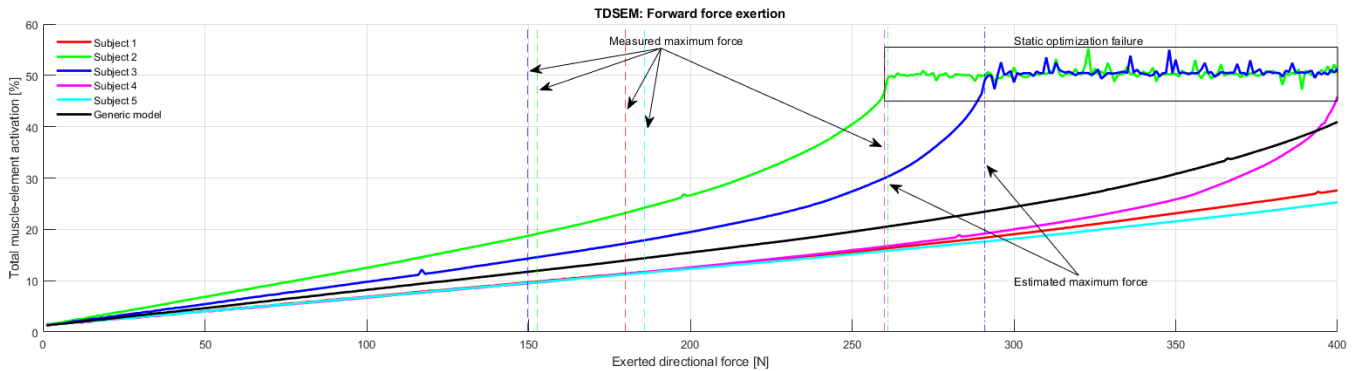


Fig. 5: Plot illustrating the result of the indirect validation method for the scaled- and generic version of the thoracoscapular Delft shoulder and elbow model (TDSEM). Models were tasked to exert force in a forward direction. The horizontal axis denotes prescribed forward force exertion. The vertical axis denotes the percentual summed muscle activation – 100% indicates all muscle elements maximally contracting simultaneously. Line color indicates the subject. Solid lines indicate summed muscle activation for a given model at a prescribed directional force. Dashed vertical lines indicate measured subject-specific maximum force exertion values. Dashed-dotted lines indicate subject-specific maximum force estimated with the indirect validation method. No estimations are made for subjects 1, 4, and 5, and the generic model, as static optimization failure did not occur for these models in the sampled range of 1 to 400N.

in the DSEM constrains two points on the scapula – the trigonum spinae and the angulus inferior – to a different ellipsoid surface [72]. The ST joint in the TDSEM constrains one point – the mid-point of the scapula – to an ellipsoid surface [17] (Figure 2b). Second, the direction of resulting GH joint-force at all evaluated instances is constrained in the DSEM such that it is directed into the glenoid surface to maintain stability [16], [69]. Such a constraint is not present in the TDSEM or TSM. Third, ligament elements present in the DSEM are not included in the TDSEM or TSM. Fourth, results obtained from muscle-driven simulations with the DSEM employ a different load-sharing strategy, minimizing energy expenditure [102], [103] rather than squared activation. Changes in load-sharing strategy are highly influential to obtained results [102], [104], [105]. Changes in joint-forces as a result of altering load-sharing strategy are of similar magnitude as changes from muscle-strength scaling [5].

B. Subject-specific scaling tools

1) *Geometric scaling*: Most subject-specific models created in this study achieve the desired accuracy in terms of RMS marker error (≤ 2 cm) and segmental length errors ($\leq 5\%$). The fit of the geometric scaling procedure presented is mainly dependent on the accuracy of provided marker-data. Use of this method over the native OpenSim scaling tool is recommended when scaling the TSM and TDSEM as ST joint properties scale proportionally to the thoracic segment. These greatly influence kinematic fits obtainable with scaled models. For this scaling, it is recommended to use marker data that spans a substantial amount of the subject’s RoM. The posed method is likely best suited to be used with data from individually placed reflective markers. In general, this method provides an easy-to-use marker-based scaling method that sets a baseline for TSM and TDSEM scaling performance.

Geometric scaling can be further improved by:

- Using a model scaled with OpenSim’s native scaling tool as input to the algorithm, rather than the un-scaled generic model. This could lead to the optimizer converging to a better minimum or reduce optimization times.
- Only adjust scale-factors from the native scaling tool that are trusted least. The scale-factors of the thorax, for instance. This is dependent on the confidence in the accuracy of marker-data used. For scapular scaling using palpated bony landmarks, the inclusion of the processus coracoideus is known to improve scaling performance [55].
- ST joint parameters can be further refined in a scaled model for motions involving significant deformations of the thorax, like lateral flexion [14].

2) *Muscle-length scaling*: The muscle-length scaling algorithm presented adjusts the tool presented by Modenesse et al. [59] to function with the TSM and TDSEM, and the latest version of the OpenSim software. These algorithms are needed to maintain the force-generating capacity of muscle-elements throughout the full RoM after geometric scaling, which is insufficiently done by proportionally adjusting optimal fiber- and tendon slack length properties [58]–[60]. The desired optimization fit is reached with scaled versions of TSM and TDSEM and is comparable to- or better than the reported fit in other works employing similar algorithms [18], [59], [60].

It is recommended to always use the presented algorithm after geometrically scaling the generic TSM or TDSEM. When scaling these models, the two-step algorithm should be exclusively used due to overestimations of tendon slack length made with the default scaling algorithm for muscles crossing the ST joint. A limit value for the number of model-poses is introduced to prevent redundant sampling of muscle-properties for muscle-elements spanning a large number of DoFs. This limit value needs to be selected

based on hardware limitations, time available for the scaling procedure, and the number of muscle-elements in the model.

3) *Muscle-strength scaling*: The muscle-strength scaling method is based on the strong linear relationship between the total muscle volume in the upper-extremity and the average maximum force exerted by a subject [65]. A difference with the uniform method in Bolsterlee et al. [65] is that muscle-element volume is scaled based on the optimal fiber length estimated with muscle-length scaling, rather than a proportionally scaled optimal fiber length value. The resulting differences in scaled maximum isometric muscle-element strength are small. Scaled maximum isometric muscle-element strength values obtained with either method cannot be validated directly.

Applicability of this scaling method when modelling specifically trained athletes or patients is debatable. Limitations come from the enhanced or impaired ability to exert force in specific directions, or less uniform distributions of muscle tissue resulting from specific hypertrophic- or atrophic adaptations in these subjects [44], [106], [107]. The applicability of the used linear relationship to these groups of subjects has not been evaluated.

4) *Inertial scaling*: The inertial scaling method presented is based on the same correlation as muscle-strength scaling and uniformly adjust segmental mass and rotational inertia based on estimated total muscle-volume in the upper-extremity. Inertial scaling is not present in the uniform scaling method by Bolsterlee et al. [65]. As inter-individual in segmental mass and inertia resulting from fat or bone is not taken into account, scaled values can be considered rough estimations. These estimations are assumed more similar to actual subject-specific inertial properties than the generic ones in most cases. This was not validated for the subjects modelled.

More accurate estimates of inertial properties can be obtained using the method by Pataky et al. [108], or DXA measurements [44], [106]. This is worthwhile when studying tasks more sensitive to inertial parameters [30], [36], or when modelling specifically trained athletes or patients whose mass distribution might substantially deviate from the generic model's.

C. Indirect validation method

The indirect validation method presented in this study attempts to recreate the maximum isometric force trials by Bolsterlee et al. [65] using a SO procedure. Whilst the method did function as intended, few estimations could be made in the ranges of directional forces prescribed: 1 to 400N. Estimations that were made all grossly overestimated subject-specific maximum forces measured.

Errors in the subject-specific models include incorrect estimation of the subject's pose during the trial, incorrect subject-specific scaling, and errors present in the generic model. Of these, errors in the generic model are likely most influential. Isometric force-exertion at the hand is also limited

by muscles crossing the wrist, rather than upper-extremity musculature only. Measured peak voluntary moments of wrist- flexion and extension, and radial- and ulnar deviation [109] are smaller than corresponding torque-directions measured at the handle by Bolsterlee [65] and likely resulted in some movement of the subject. The inclusion of muscles crossing the wrist will likely influence failure loads in directions primarily loading these DoFs: leftwards, rightwards, upwards, and downwards. Peak forearm- pronation and supination torques measured [110] are highly similar in magnitude to the corresponding torque-direction measured. Furthermore, the absence of a constraint to maintain GH stability allows reaction forces in the GH joint that would cause luxation.

During the simulations, the trunk of each subject-specific model is fully constrained. During actual measurements, each subject's trunk would start rotating or translating if sufficient force was exerted upon it, which was not allowed in simulation. Torques measured at the handle during the trials by Bolsterlee [65] are of similar magnitude as maximum isometric trunk torques reported [111]. Thus, forces exerted during measurements might have been limited by the subject's ability to isometrically oppose reaction forces and torques exerted onto the trunk by the arm. This contradicts the made assumption that forces exerted onto the handle are only limited by the strength of upper-extremity musculature.

It is not easy for untrained individuals to maximally contract muscles, or to determine the most effective method of exerting directional force without extensive practice or feedback on performance. This can also have contributed to the overestimation of maximum force made with the subject-specific models.

The discrepancy between measured- and estimated maximum directional forces can be reduced by; improving generic models through the inclusion of a wrist model and a GH stability constraint, and altering the measurement procedure by; constraining the subject's trunk during measurement, recording their pose, and using trained individuals. Alternatively, maximum isometric force polytopes, similar to Hernandez et al. [112], can be measured. In that case, the number of maximum force directions tested increases from 6 to 26.

D. Future recommendations

It is worthwhile to fully reconstruct the generic TDSEM model from DSEM data before making it available on the SimTK platform. With this, previously mentioned problems with the implementation of muscle-attachments and wrapping geometries in the DAS model are likely resolved. This should be a priority as it limits the validity of results generated with TDSEM-based models. This would also allow the similarity between the TDSEM and DSEM to be increased by implementing an identical closed-loop kinematic structure. Ligament elements from the DSEM can be integrated using the ligament-model by Blankevoort et. al [113], available in OpenSim. To further improve the similarity between TDSEM and DSEM, the effect of including the GH stability constraint

and using an energy-expenditure-based load-sharing criterion on muscle-driven simulation results should be evaluated. Both of these can be implemented in MATLAB – similar to Akhavanfar et al. [114] –, OpenSim MOCO [115] or SCONE [116], [117].

Subject-specific scaling methods can be improved further with methods mentioned earlier in this section. These improvements should be made based on the task and subject studied.

The indirect validation method needs to be improved before it can be used by future modellers as part of their methodology to (in-)validate their subject-specific models. For this, the effect on the measured maximum force at the handle of constraining the subject’s trunk during measurement, and allowing the subjects to practice the task should be quantified. Within the set of subjects, strength-trained individuals – experienced with maximally contracting muscles – should be included. During measurements, the pose of each subject needs to be recorded. Potentially, these measures can eliminate much of the discrepancies observed in the present study. Within the simulation, the reconstructed generic TDSEM recommended previously should be used to create subject-specific models.

V. CONCLUSION

The purpose of this study is to enable future OpenSim users to perform muscle-driven simulations with adequately scaled, subject-specific upper-extremity models. For this, a generic upper-extremity model; the TDSEM, a set of easy-to-use subject-specific scaling methods, and a method to indirectly validate subject-specific models by predicting maximum subject-exerted forces at the hand are developed.

The TDSEM successfully integrates the closed-loop kinematic structure of the TSM into the DAS model and is usable with all muscle-driven analyses available in OpenSim. Subject-specific versions of the TDSEM were able to achieve a kinematic fit comparable to subject-specific versions of the TSM, whilst better introducing measured between-subject proportionality in simulations of maximum force trials. It is worthwhile to reconstruct the TDSEM from DSEM data to correct errors found in the adopted DAS model and include ligament elements. Future muscle-driven simulations performed herewith should use a GH stability constraint and a load-sharing algorithm based on energy-expenditure for results more similar to the DSEM.

The subject-specific scaling methods developed were able to reach both the desired IK marker-error and muscle-length-parameter optimization fit. Muscle-strength- and inertial scaling results could not be validated, but likely decrease the discrepancy between generic- and actual values as this scaling is rarely performed. Presented methods are recommended over OpenSim’s native methods when scaling either the TSM or the TDSEM.

The indirect validation method developed was not able to (in-)validate subject-specific models presented in this study, due to large overestimations of subject-specific forces measured, regardless of the subject modelled or generic model

used. To improve the usability of this method, the effect on measured forces of constraining the subject’s torso during measurement, allowing for task-specific practice, and include trained subjects should be evaluated. The subject’s pose during these trials should also be recorded. Combined with the GH stability constraint, this can potentially eliminate much of the currently present discrepancies in future studies.

REFERENCES

- [1] F Steenbrink, J H De Groot, H E J Veeger, F C T van der Helm, and P M Rozing. Glenohumeral stability in simulated rotator cuff tears. *Journal of biomechanics*, 42(11):1740–1745, 2009.
- [2] Hans Kainz, Hoa X. Hoang, Chris Stockton, Roslyn R. Boyd, David G. Lloyd, and Christopher P. Carty. Accuracy and reliability of marker-based approaches to scale the pelvis, thigh, and shank segments in musculoskeletal models. *Journal of Applied Biomechanics*, 33(5), 2017.
- [3] Mariska Wesseling, Friedl De Groote, Christophe Meyer, Kristoff Corten, Jean-Pierre Simon, Kaat Desloovere, and Ilse Jonkers. Subject-specific musculoskeletal modelling in patients before and after total hip arthroplasty. *Computer methods in biomechanics and biomedical engineering*, 19(15):1683–1691, 2016.
- [4] Benjamin J Fregly. Design of optimal treatments for neuromusculoskeletal disorders using patient-specific multibody dynamic models. *International journal for computational vision and biomechanics*, 2(2):145, 2009.
- [5] Bart Bolsterlee. *Subject-specific upper extremity modelling*. Doctoral thesis, Technische Universiteit Delft, 2014.
- [6] Scott L Delp, Frank C Anderson, Allison S Arnold, Peter Loan, Ayman Habib, Chand T John, Eran Guendelman, and Darryl G Thelen. OpenSim: Open-Source Software to Create and Analyze Dynamic Simulations of Movement. *IEEE TRANSACTIONS ON BIOMEDICAL ENGINEERING*, 54(11):1940–1950, 2007.
- [7] Ajay Seth, Michael Sherman, Jeffrey A. Reinbolt, and Scott L. Delp. OpenSim: A musculoskeletal modeling and simulation framework for in silico investigations and exchange. *Procedia IUTAM*, 2:212–232, 2011.
- [8] Ajay Seth, Jennifer L Hicks, Thomas K Uchida, Ayman Habib, Christopher L Dembia, James J Dunne, Carmichael F Ong, Matthew S DeMers, Apoorva Rajagopal, Matthew Millard, Samuel R Hamner, Edith M Arnold, Jennifer R Yong, Shrinidhi K Lakshminanth, Michael A Sherman, Joy P Ku, and Scott L Delp. OpenSim: Simulating musculoskeletal dynamics and neuromuscular control to study human and animal movement. *PLOS Computational Biology*, 14(7):1–20, 2018.
- [9] John Rasmussen, Michael Damsgaard, Egidijus Surma, Søren T Christensen, Mark de Zee, and Vit Vondrak. Anybody-a software system for ergonomic optimization. In *Fifth World Congress on Structural and Multidisciplinary Optimization*, volume 4. Citeseer, 2003.
- [10] Michael Damsgaard, John Rasmussen, Søren Tørholm Christensen, Egidijus Surma, and Mark De Zee. Analysis of musculoskeletal systems in the AnyBody Modeling System. *Simulation Modelling Practice and Theory*, 14(8):1100–1111, 2006.
- [11] Jingzhou Yang, Xuemei Feng, Joo H Kim, and Sudhakar Rajulu. Review of biomechanical models for human shoulder complex. *International Journal of Human Factors Modelling and Simulation*, 1(3):271–293, 2010.
- [12] Raphael Dumas, Michael Skipper Andersen, and Mickael Begon. What are the joint models used in multibody kinematic optimisation for the estimation of human joint kinematics? a review. In *Proceedings of the 4th International Digital Human Modeling Symposium*, 2016.
- [13] Joe A.I. Prinold, Milad Masjedi, Garth R. Johnson, and Anthony M.J. Bull. Musculoskeletal shoulder models: A technical review and proposals for research foci. *Proceedings of the Institution of Mechanical Engineers, Part H: Journal of Engineering in Medicine*, 227(10):1041–1057, 2013.
- [14] Ajay Seth, Meilin Dong, Ricardo Matias, and Scott Delp. Muscle contributions to upper-extremity movement and work from a musculoskeletal model of the human shoulder. *Frontiers in Neurobotics*, 13(November):1–9, 2019.

- [15] Mary D. Klein Breteler, Cornelis W. Spoor, and Frans C.T. Van Der Helm. Measuring muscle and joint geometry parameters of a shoulder for modeling purposes. *Journal of Biomechanics*, 32(11):1191–1197, 1999.
- [16] A Asadi Nikooyan, H E J Veeger, E K J Chadwick, M Praagman, and Frans C T van der Helm. Development of a comprehensive musculoskeletal model of the shoulder and elbow. *Medical & biological engineering & computing*, 49(12):1425–1435, 2011.
- [17] Ajay Seth, Ricardo Matias, António P Veloso, and Scott L Delp. A biomechanical model of the scapulothoracic joint to accurately capture scapular kinematics during shoulder movements. *PLoS one*, 11(1):e0141028, 2016.
- [18] Wen Wu, Peter V.S. Lee, Adam L. Bryant, Mary Galea, and David C. Ackland. Subject-specific musculoskeletal modeling in the evaluation of shoulder muscle and joint function. *Journal of Biomechanics*, 49(15):3626–3634, 2016.
- [19] Katherine R. Saul, Xiao Hu, Craig M. Goehler, Meghan E. Vidt, Melissa Daly, Anca Velisar, and Wendy M. Murray. Benchmarking of dynamic simulation predictions in two software platforms using an upper limb musculoskeletal model. *Computer Methods in Biomechanics and Biomedical Engineering*, 18(13), 2015.
- [20] Edward K Chadwick, Dimitra Blana, Robert F Kirsch, and Antonie J Van Den Bogert. IEEE TRANSACTIONS ON BIOMEDICAL ENGINEERING Real-Time Simulation of Three-Dimensional Shoulder Girdle and Arm Dynamics. 61(7):1–10, 2014.
- [21] Antonie J. Van Den Bogert, Dimitra Blana, and Dieter Heinrich. Implicit methods for efficient musculoskeletal simulation and optimal control. *Procedia IUTAM*, 2:297–316, 2011.
- [22] Dimitra Blana, Juan G Hincapie, Edward K Chadwick, and Robert F Kirsch. A musculoskeletal model of the upper extremity for use in the development of neuroprosthetic systems. *Journal of biomechanics*, 41(8):1714–1721, 2008.
- [23] R E Hughes and K-N An. Monte Carlo simulation of a planar shoulder model. *Medical and Biological Engineering and Computing*, 35(5):544–548, 1997.
- [24] David C. Ackland, Yi Chung Lin, and Marcus G. Pandy. Sensitivity of model predictions of muscle function to changes in moment arms and muscle-tendon properties: A Monte-Carlo analysis. *Journal of Biomechanics*, 45(8):1463–1471, 2012.
- [25] P. Bujalski, J. Martins, and L. Stirling. A Monte Carlo analysis of muscle force estimation sensitivity to muscle-tendon properties using a Hill-based muscle model. *Journal of Biomechanics*, 79:67–77, 2018.
- [26] F. De Groot, A. Van Campen, I. Jonkers, and J. De Schutter. Sensitivity of dynamic simulations of gait and dynamometer experiments to hill muscle model parameters of knee flexors and extensors. *Journal of Biomechanics*, 43(10):1876–1883, 2010.
- [27] V. Carbone, M. M. van der Krogt, H. F. J. M. Koopman, and N. Verdonchot. Sensitivity of subject-specific models to errors in musculo-skeletal geometry. *Journal of Biomechanics*, 45(14):2476–2480, sep 2012.
- [28] Carol Y. Scovil and Janet L. Ronsky. Sensitivity of a Hill-based muscle model to perturbations in model parameters. *Journal of Biomechanics*, 39(11):2055–2063, 2006.
- [29] Christian Redl, Margit Gfoehler, and Marcus G. Pandy. Sensitivity of muscle force estimates to variations in muscle-tendon properties. *Human Movement Science*, 26(2):306–319, apr 2007.
- [30] Tien Tuan Dao, Frédéric Marin, and Marie Christine Hobatho. Sensitivity of the anthropometrical and geometrical parameters of the bones and muscles on a musculoskeletal model of the lower limbs. *Proceedings of the 31st Annual International Conference of the IEEE Engineering in Medicine and Biology Society: Engineering the Future of Biomedicine, EMBC 2009*, pages 5251–5254, 2009.
- [31] Saulo Martelli, Giordano Valente, Marco Viceconti, and Fulvia Taddei. Sensitivity of a subject-specific musculoskeletal model to the uncertainties on the joint axes location. *Computer Methods in Biomechanics and Biomedical Engineering*, 18(14):1555–1563, 2015.
- [32] G. Lenaerts, F. De Groot, B. Demeulenaere, M. Mulier, G. Van der Perre, A. Spaepen, and I. Jonkers. Subject-specific hip geometry affects predicted hip joint contact forces during gait. *Journal of Biomechanics*, 41(6):1243–1252, 2008.
- [33] Giordano Valente, Lorenzo Pitto, Debora Testi, Ajay Seth, Scott L Delp, Rita Stagni, Marco Viceconti, and Fulvia Taddei. Are subject-specific musculoskeletal models robust to the uncertainties in parameter identification? *PLoS One*, 9(11):e112625, 2014.
- [34] Giordano Valente, Lorenzo Pitto, Rita Stagni, and Fulvia Taddei. Effect of lower-limb joint models on subject-specific musculoskeletal models and simulations of daily motor activities. *Journal of Biomechanics*, 48(16):4198–4205, 2015.
- [35] Casey A. Myers, Peter J. Laz, Kevin B. Shelburne, and Bradley S. Davidson. A Probabilistic Approach to Quantify the Impact of Uncertainty Propagation in Musculoskeletal Simulations. *Annals of Biomedical Engineering*, 43(5), 2015.
- [36] Guillaume Rao, David Amarantini, Eric Berton, and Daniel Favier. Influence of body segments’ parameters estimation models on inverse dynamics solutions during gait. *Journal of biomechanics*, 39(8):1531–1536, 2006.
- [37] Georg N. Duda, Doris Brand, Sabine Freitag, Werner Lierse, and Erich Schneider. Variability of femoral muscle attachments. *Journal of Biomechanics*, 29(9):1185–1190, sep 1996.
- [38] Lennart Scheys, Kaat Desloovere, Paul Suetens, and Ilse Jonkers. Level of subject-specific detail in musculoskeletal models affects hip moment arm length calculation during gait in pediatric subjects with increased femoral anteversion. *Journal of Biomechanics*, 44(7):1346–1353, 2011.
- [39] Saikat Pal, Joseph E Langenderfer, Joshua Q Stowe, Peter J Laz, Anthony J Petrella, and Paul J Rullkoetter. Probabilistic Modeling of Knee Muscle Moment Arms: Effects of Methods, Origin–Insertion, and Kinematic Variability. *Annals of Biomedical Engineering*, 35(9):1632–1642, sep 2007.
- [40] Scott R McGarvey, Bernard F Morrey, Linda J Askew, and K N An. Reliability of isometric strength testing. Temporal factors and strength variation. *Clinical orthopaedics and related research*, (185):301–305, 1984.
- [41] Katherine R S Holzbaur, Wendy M. Murray, Garry E. Gold, and Scott L. Delp. Upper limb muscle volumes in adult subjects. *Journal of Biomechanics*, 40(4):742–749, 2007.
- [42] D J Pearsall and P A Costigan. The effect of segment parameter error on gait analysis results. *Gait & Posture*, 9(3):173–183, 1999.
- [43] Amy R Lewis, William S P Robertson, Elissa J Phillips, Paul N Grimshaw, and Marc Portus. The Effects of Personalized Versus Generic Scaling of Body Segment Masses on Joint Torques During Stationary Wheelchair Racing. *Journal of Biomechanical Engineering*, 141(10), 2019.
- [44] Marcel Rossi, Andrew Lyttle, EL-SALLAM Amar, Nat Benjanuvatra, and Brian Blanksby. Body segment inertial parameters of elite swimmers using DXA and indirect methods. *Journal of sports science & medicine*, 12(4):761, 2013.
- [45] Silvia S. Blemker, Deanna S. Asakawa, Garry E. Gold, and Scott L. Delp. Image-based musculoskeletal modeling: Applications, advances, and future opportunities. *Journal of Magnetic Resonance Imaging*, 25(2):441–451, 2007.
- [46] Lennart Scheys, Anja Van Campenhout, Arthur Spaepen, Paul Suetens, and Ilse Jonkers. Personalized MR-based musculoskeletal models compared to rescaled generic models in the presence of increased femoral anteversion: Effect on hip moment arm lengths. *Gait and Posture*, 28(3):358–365, 2008.
- [47] Allison S. Arnold, Silvia Salinas, Deanna J. Asakawa, and Scott L. Delp. Accuracy of muscle moment arms estimated from MRI-based musculoskeletal models of the lower extremity. *Computer Aided Surgery*, 5(2):108–119, 2000.
- [48] Jérôme Schmid, Anders Sandholm, François Chung, Daniel Thalmann, Hervé Delingette, and Nadia Magnenat-Thalmann. Musculoskeletal simulation model generation from MRI data sets and motion capture data. In *Recent advances in the 3D physiological human*, pages 3–19. Springer, 2009.
- [49] T Fukunaga, R R Roy, F G Shellock, J A Hodgson, M K Day, P L Lee, H Kwong-Fu, and V R Edgerton. Physiological cross-sectional area of human leg muscles based on magnetic resonance imaging. *Journal of orthopaedic research*, 10(6):926–934, 1992.
- [50] B.L. Kaptein. *Towards in vivo parameter estimation for a musculoskeletal model of the human shoulder*. PhD thesis, TU Delft, 1999.
- [51] B.L. Kaptein and F.C.T. van der Helm. Estimating muscle attachment contours by transforming geometrical bone models. *Journal of Biomechanics*, 37(3):263–273, mar 2004.
- [52] P. Pellikaan, M.M. van der Krogt, V. Carbone, R. Fluit, L.M. Vigneron, J. Van Deun, N. Verdonchot, and H.F.J.M. Koopman. Evaluation of a morphing based method to estimate muscle at-

- attachment sites of the lower extremity. *Journal of Biomechanics*, 47(5):1144–1150, mar 2014.
- [53] Sonia Duprey, Alexandre Naaim, Florent Moissenet, Mickaël Begon, and Laurence Chèze. Kinematic models of the upper limb joints for multibody kinematics optimisation: An overview. *Journal of Biomechanics*, 62:87–94, 2017.
- [54] Morten Enemark Lund, Michael Skipper Andersen, Mark de Zee, and John Rasmussen. Scaling of musculoskeletal models from static and dynamic trials. *International Biomechanics*, 2(1), 2015.
- [55] Bart Bolsterlee and Amir Abbas Zadpoor. Transformation methods for estimation of subject-specific scapular muscle attachment sites. *Computer methods in biomechanics and biomedical engineering*, 17(13):1492–1501, 2014.
- [56] Archibald Vivian Hill. The heat of shortening and the dynamic constants of muscle. *Proceedings of the Royal Society of London. Series B - Biological Sciences*, 126(843):136–195, 1938.
- [57] Felix E Zajac. Muscle and tendon: properties, models, scaling, and application to biomechanics and motor control. *Critical reviews in biomedical engineering*, 17(4):359–411, 1989.
- [58] C. R. Winby, D. G. Lloyd, and T. B. Kirk. Evaluation of different analytical methods for subject-specific scaling of musculotendon parameters. *Journal of Biomechanics*, 41(8):1682–1688, 2008.
- [59] Luca Modenese, Elena Ceseracciu, Monica Reggiani, and David G. Lloyd. Estimation of musculotendon parameters for scaled and subject specific musculoskeletal models using an optimization technique. *Journal of Biomechanics*, 49(2):141–148, 2016.
- [60] Pablo Peñas. *Parameter Scaling Protocol for Upper-limb Musculoskeletal Models*. Master thesis, Technische Universiteit Delft, 2019.
- [61] Frederik Heinen, Morten E. Lund, John Rasmussen, and Mark De Zee. Muscle-tendon unit scaling methods of Hill-type musculoskeletal models: An overview. *Proceedings of the Institution of Mechanical Engineers, Part H: Journal of Engineering in Medicine*, 230(10):976–984, 2016.
- [62] Frederik Heinen, Søren N Sørensen, Mark King, Martin Lewis, Morten Enemark Lund, John Rasmussen, and Mark de Zee. Muscle-tendon unit parameter estimation of a Hill-type musculoskeletal model based on experimentally obtained subject-specific torque profiles. *Journal of biomechanical engineering*, 141(6):61005, 2019.
- [63] Reinhard Hainisch, Margit Gfoehler, M. Zubayer-UI-Karim, and Marcus G. Pandy. Method for determining musculotendon parameters in subject-specific musculoskeletal models of children developed from MRI data. *Multibody System Dynamics*, 28(1-2):143–156, 2012.
- [64] Geoffrey G Handsfield, Craig H Meyer, Joseph M Hart, Mark F Abel, and Silvia S Blemker. Relationships of 35 lower limb muscles to height and body mass quantified using MRI. *Journal of biomechanics*, 47(3):631–638, 2014.
- [65] Bart Bolsterlee, Alistair N. Vardy, Frans C.T. van der Helm, and H. E.J. (DirkJan) Veeger. The effect of scaling physiological cross-sectional area on musculoskeletal model predictions. *Journal of Biomechanics*, 48(10):1760–1768, 2015.
- [66] Benjamin Goulsard de Monsabert, G. Rao, A. Gay, E. Berton, and L. Vigouroux. A scaling method to individualise muscle force capacities in musculoskeletal models of the hand and wrist using isometric strength measurements. *Medical and Biological Engineering and Computing*, 55(12):2227–2244, 2017.
- [67] Richard N Hinrichs. Regression equations to predict segmental moments of inertia from anthropometric measurements: an extension of the data of Chandler et al.(1975). *Journal of Biomechanics*, 18(8):621–624, 1985.
- [68] Maurice R Yeadon and M Morlock. The appropriate use of regression equations for the estimation of segmental inertia parameters. *Journal of biomechanics*, 22(6-7):683–689, 1989.
- [69] H. E.J. Veeger and F. C.T. van der Helm. Shoulder function: The perfect compromise between mobility and stability. *Journal of Biomechanics*, 40(10):2119–2129, 2007.
- [70] A. A. Nikooyan, H. E.J. Veeger, P. Westerhoff, F. Graichen, G. Bergmann, and F. C.T. van der Helm. Validation of the Delft Shoulder and Elbow Model using in-vivo glenohumeral joint contact forces. *Journal of Biomechanics*, 43(15):3007–3014, 2010.
- [71] F. C.T. van der Helm and R. Veenbaas. Modelling the mechanical effect of muscles with large attachment sites: Application to the shoulder mechanism. *Journal of Biomechanics*, 24(12):1151–1163, jan 1991.
- [72] Frans C T der Helm. A finite element musculoskeletal model of the shoulder mechanism. *Journal of biomechanics*, 27(5):551–569, 1994.
- [73] P. L. Powell, R. R. Roy, P. Kanim, M. A. Bello, and V. R. Edgerton. Predictability of skeletal muscle tension from architectural determinations in guinea pig hindlimbs. *Journal of Applied Physiology Respiratory Environmental and Exercise Physiology*, 57(6):1715–1721, 1984.
- [74] Florent Moissenet, Laurence Chèze, and Raphaël Dumas. A 3D lower limb musculoskeletal model for simultaneous estimation of musculotendon, joint contact, ligament and bone forces during gait. *Journal of Biomechanics*, 47(1):50–58, 2014.
- [75] M. O. Heller, G. Bergmann, G. Deuretzbacher, L. Dürselen, M. Pohl, L. Claes, N. P. Haas, and G. N. Duda. Musculo-skeletal loading conditions at the hip during walking and stair climbing. *Journal of Biomechanics*, 34(7):883–893, 2001.
- [76] Pauline Gerus, Massimo Sartori, Thor F. Besier, Benjamin J. Fregly, Scott L. Delp, Scott A. Banks, Marcus G. Pandy, Darryl D. D’Lima, and David G. Lloyd. Subject-specific knee joint geometry improves predictions of medial tibiofemoral contact forces. *Journal of Biomechanics*, 46(16):2778–2786, 2013.
- [77] William R. Taylor, Pascal Schütz, Georg Bergmann, Renate List, Barbara Postolka, Marco Hitz, Jörn Dymke, Philipp Damm, Georg Duda, Hans Gerber, Verena Schwachmeyer, Seyyed Hamed Hosseini Nasab, Adam Trepczynski, and Ines Kutzner. A comprehensive assessment of the musculoskeletal system: The CAMS-Knee data set. *Journal of Biomechanics*, 65, 2017.
- [78] Massimo Sartori, Monica Reggiani, Dario Farina, and David G Lloyd. EMG-Driven Forward-Dynamic Estimation of Muscle Force and Joint Moment about Multiple Degrees of Freedom in the Human Lower Extremity. *PLOS ONE*, 7(12):1–11, 2012.
- [79] David G. Lloyd and Thor F. Besier. An EMG-driven musculoskeletal model to estimate muscle forces and knee joint moments in vivo. *Journal of Biomechanics*, 36(6):765–776, 2003.
- [80] Andrew J. Meyer,Carolynn Patten, and Benjamin J. Fregly. Lower extremity EMG-driven modeling of walking with automated adjustment of musculoskeletal geometry. *PLoS ONE*, 12(7), 2017.
- [81] Terry K K Koo and Arthur F T Mak. Feasibility of using EMG driven neuromusculoskeletal model for prediction of dynamic movement of the elbow. *Journal of electromyography and kinesiology*, 15(1):12–26, 2005.
- [82] Ursula Trinler, Kristen Hollands, Richard Jones, and Richard Baker. A systematic review of approaches to modelling lower limb muscle forces during gait: Applicability to clinical gait analyses. *Gait & Posture*, 61:353–361, mar 2018.
- [83] Antoine Falisse, Sam Van Rossom, Ilse Jonkers, and Friedl De Groot. EMG-Driven Optimal Estimation of Subject-SPECIFIC Hill Model Muscle-Tendon Parameters of the Knee Joint Actuators. *IEEE Transactions on Biomedical Engineering*, 64(9), 2017.
- [84] Luciano Luporini Menegaldo and Liliam Fernandes de Oliveira. Effect of muscle model parameter scaling for isometric plantar flexion torque prediction. *Journal of Biomechanics*, 42(15):2597–2601, 2009.
- [85] B Bigland-Ritchie, R Johansson, O C Lippold, and J J Woods. Contractile speed and EMG changes during fatigue of sustained maximal voluntary contractions. *Journal of neurophysiology*, 50(1):313–324, 1983.
- [86] Dario Farina, Roberto Merletti, and Roger M Enoka. The extraction of neural strategies from the surface EMG. *Journal of applied physiology*, 96(4):1486–1495, 2004.
- [87] Jennifer L. Hicks, Thomas K. Uchida, Ajay Seth, Apoorva Rajagopal, and Scott L. Delp. Is My Model Good Enough? Best Practices for Verification and Validation of Musculoskeletal Models and Simulations of Movement, 2015.
- [88] Bart Bolsterlee, H E J Veeger, and Frans C T van der Helm. Modelling clavicular and scapular kinematics: from measurement to simulation. *Medical & biological engineering & computing*, 52(3):283–291, 2014.
- [89] G M Pronk and F C T der Helm. The palpator: an instrument for measuring the positions of bones in three dimensions. *Journal of medical engineering & technology*, 15(1):15–20, 1991.
- [90] Andrea Giovanni Cutti, Gabriele Paolini, Marco Troncosi, Angelo Cappello, and Angelo Davalli. Soft tissue artefact assessment in humeral axial rotation. *Gait & posture*, 21(3):341–349, 2005.
- [91] Kazuhisa Matsui, Kazushi Shimada, and Paul D Andrew. Deviation of skin marker from bone target during movement of the scapula. *Journal of Orthopaedic Science*, 11(2):180–184, 2006.

- [92] Ge Wu, Frans C.T. Van Der Helm, H. E.J. Veeger, Mohsen Makhssous, Peter Van Roy, Carolyn Anglin, Jochem Nagels, Andrew R. Karduna, Kevin McQuade, Xuguang Wang, Frederick W. Werner, and Bryan Buchholz. ISB recommendation on definitions of joint coordinate systems of various joints for the reporting of human joint motion - Part II: Shoulder, elbow, wrist and hand. *Journal of Biomechanics*, 38(5):981–992, 2005.
- [93] Katherine R S Holzbaur, Wendy M Murray, and Scott L Delp. A model of the upper extremity for simulating musculoskeletal surgery and analyzing neuromuscular control. *Annals of biomedical engineering*, 33(6):829–840, 2005.
- [94] David C. Ackland, Ponnaren Pak, Martin Richardson, and Marcus G. Pandy. Moment arms of the muscles crossing the anatomical shoulder. *Journal of Anatomy*, 213(4):383–390, 2008.
- [95] Lisa M Schutte, Mary M Rodgers, F E Zajac, and Roger M Glaser. Improving the efficacy of electrical stimulation-induced leg cycle ergometry: an analysis based on a dynamic musculoskeletal model. *IEEE Transactions on Rehabilitation Engineering*, 1(2):109–125, 1993.
- [96] Matthew Millard, Thomas Uchida, Ajay Seth, and Scott L Delp. Flexing computational muscle: modeling and simulation of musculotendon dynamics. *Journal of biomechanical engineering*, 135(2), 2013.
- [97] The Mathworks, Inc., Natick, Massachusetts. *MATLAB version 9.6.0.1150989 (R2019a) Update 4*, 2019.
- [98] H E J Veeger, Bing Yu, and Kai Nan An. Orientation of axes in the elbow and forearm for biomechanical modeling. In *Proceedings of the First Conference of the International Shoulder Group*. Shaker Publishing, Maastricht, pages 83–87. Citeseer, 1996.
- [99] M Stokdijk, J Nagels, and P M Rozing. The glenohumeral joint rotation centre in vivo. *Journal of Biomechanics*, 33(12):1629–1636, 2000.
- [100] Samuel R. Ward, Carolyn M. Eng, Laura H. Smallwood, and Richard L. Lieber. Are current measurements of lower extremity muscle architecture accurate? *Clinical Orthopaedics and Related Research*, 467(4):1074–1082, 2009.
- [101] Joseph Langenderfer, Seth A. Jerabek, Vijay B. Thangamani, John E. Kuhn, and Richard E. Hughes. Musculoskeletal parameters of muscles crossing the shoulder and elbow and the effect of sarcomere length sample size on estimation of optimal muscle length. *Clinical Biomechanics*, 19(7):664–670, 2004.
- [102] M Praagman, E K J Chadwick, F C T Van Der Helm, and H E J Veeger. The relationship between two different mechanical cost functions and muscle oxygen consumption. *Journal of biomechanics*, 39(4):758–765, 2006.
- [103] M Praagman. *Muscle load sharing: An energy-based approach*. PhD thesis, Vrije Universiteit Amsterdam, 2008.
- [104] Magdalena Zuk, Malgorzata Syczewska, and Celina Pezowicz. Influence of uncertainty in selected musculoskeletal model parameters on muscle forces estimated in inverse dynamics-based static optimization and hybrid approach. *Journal of Biomechanical Engineering*, 140(12), 2018.
- [105] Ross H Miller, Brian R Umberger, Joseph Hamill, and Graham E Caldwell. Evaluation of the minimum energy hypothesis and other potential optimality criteria for human running. *Proceedings of the Royal Society B: Biological Sciences*, 279(1733):1498–1505, 2012.
- [106] Amy R Lewis, William S P Robertson, Elissa J Phillips, Paul N Grimshaw, and Marc Portus. Estimating the Maximum Isometric Force-Generating Capacity of Wheelchair Racing Athletes for Simulation Purposes. *Journal of Applied Biomechanics*, 35(5), 2019.
- [107] Brock Laschowski. *Biomechanical Modelling of Paralympic Wheelchair Curling*, 2016.
- [108] Todd C Pataky, Vladimir M Zatsiorsky, and John H Challis. A simple method to determine body segment masses in vivo: reliability, accuracy and sensitivity analysis. *Clinical Biomechanics*, 18(4):364–368, 2003.
- [109] Scott L Delp, Anita E Grierson, and Thomas S Buchanan. Maximum isometric moments generated by the wrist muscles in flexion-extension and radial-ulnar deviation. *Journal of Biomechanics*, 29(10):1371–1375, 1996.
- [110] Leonard W O’sullivan and Timothy J Gallwey. Upper-limb surface electro-myography at maximum supination and pronation torques: the effect of elbow and forearm angle. *Journal of Electromyography and Kinesiology*, 12(4):275–285, 2002.
- [111] Joseph K-F Ng, Carolyn A Richardson, Mohamad Parnianpour, and Vaughan Kippers. EMG activity of trunk muscles and torque output during isometric axial rotation exertion: a comparison between back pain patients and matched controls. *Journal of Orthopaedic Research*, 20(1):112–121, 2002.
- [112] Vincent Hernandez, Nasser Rezzoug, and Philippe Gorce. Toward isometric force capabilities evaluation by using a musculoskeletal model: Comparison with direct force measurement. *Journal of Biomechanics*, 48(12):3178–3184, 2015.
- [113] L. Blankevoort and R. Huiskes. Ligament-bone interaction in a three-dimensional model of the knee. *Journal of Biomechanical Engineering*, 113(3):263–269, 1991.
- [114] Mohammad H Akhavanfar, Scott C E Brandon, Stephen H M Brown, and Ryan B Graham. Development of a novel MATLAB-based framework for implementing mechanical joint stability constraints within OpenSim musculoskeletal models. *Journal of biomechanics*, 91:61–68, 2019.
- [115] Christopher L. Dembia, Nicholas A. Bianco, Antoine Falisse, Jennifer L. Hicks, and Scott L. Delp. OpenSim Moco: Musculoskeletal optimal control. *bioRxiv*, pages 1–25, 2019.
- [116] Thomas Geijtenbeek. SCONE: Open source software for predictive simulation of biological motion. *Journal of Open Source Software*, 4(38):1421, 2019.
- [117] Carmichael F Ong, Thomas Geijtenbeek, Jennifer L Hicks, and Scott L Delp. Predicting gait adaptations due to ankle plantarflexor muscle weakness and contracture using physics-based musculoskeletal simulations. *PLoS computational biology*, 15(10):e1006993, 2019.